Bioinformatics, 31(15), 2015, 2514–2522
doi: 10.1093/bioinformatics/btv172
Advance Access Publication Date: 25 March 2015
Original Paper

OXFORD

Systems biology

Computational modeling of the expansion of human cord blood CD133$^+$ hematopoietic stem/progenitor cells with different cytokine combinations

Francesca Gullo[1,2,†], Mark van der Garde[1,2,†], Giulia Russo[3], Marzio Pennisi[4], Santo Motta[4], Francesco Pappalardo[3,*] and Suzanne Watt[1,2,*]

[1]Stem Cell Research, Nuffield Division of Clinical Laboratory Sciences, Radcliffe Department of Medicine, University of Oxford, Oxford OX3 9DU, UK, [2]NHS Blood and Transplant Oxford, John Radcliffe Hospital, Oxford OX3 9DU, UK, [3]Department of Drug Science and [4]Department of Mathematics and Computer Science, University of Catania, 95125 Catania, Italy

*To whom correspondence should be addressed.
†The authors wish it to be known that, in their opinion, the first two authors should be regarded as Joint First Authors.
Associate Editor: Igor Jurisica

Received and revised on February 23, 2015; accepted on March 18, 2015

Abstract

Motivation: Many important problems in cell biology require dense non-linear interactions between functional modules to be considered. The importance of computer simulation in understanding cellular processes is now widely accepted, and a variety of simulation algorithms useful for studying certain subsystems have been designed. Expansion of hematopoietic stem and progenitor cells (HSC/HPC) in *ex vivo* culture with cytokines and small molecules is a method to increase the restricted numbers of stem cells found in umbilical cord blood (CB), while also enhancing the content of early engrafting neutrophil and platelet precursors. The efficacy of the expanded product depends on the composition of the cocktail of cytokines and small molecules used for culture. Testing the influence of a cytokine or small molecule on the expansion of HSC/HPC is a laborious and expensive process. We therefore developed a computational model based on cellular signaling interactions that predict the influence of a cytokine on the survival, duplication and differentiation of the CD133$^+$ HSC/HPC subset from human umbilical CB.

Results: We have used results from *in vitro* expansion cultures with different combinations of one or more cytokines to develop an ordinary differential equation model that includes the effect of cytokines on survival, duplication and differentiation of the CD133$^+$ HSC/HPC. Comparing the results of *in vitro* and *in silico* experiments, we show that the model can predict the effect of a cytokine on the fold expansion and differentiation of CB CD133$^+$ HSC/HPC after 8-day culture on a 3D scaffold.

Availability and implementation: The model is available visiting the following URL: http://www.francescopappalardo.net/Bioinformatics_CD133_Model.

Contact: francesco.pappalardo@unict.it or suzanne.watt@nhsbt.nhs.uk

Supplementary information: Supplementary data are available at *Bioinformatics* online.

1 Introduction

Hematopoietic stem cell transplantation is a potentially curative therapy for severe hematological malignancies and other severe disorders of the blood and bone marrow. Umbilical cord blood (CB) is used as an alternative for bone marrow or mobilized peripheral blood grafts, particularly when no HLA matched related or unrelated donor can be found (Ballen *et al.*, 2013; Fuchs *et al.*, 2013; Watt, 2014). However, single CB grafts have a limited number of hematopoietic stem and progenitor cells (HSC/HPC) and, when compared with mobilized peripheral blood grafts, show significantly delayed early neutrophil and platelet engraftment (Ballen *et al.*, 2013; Fuchs *et al.*, 2013; Watt, 2014). This leads to significant morbidity and mortality in myeloablated recipients in the CB transplant setting. Recent studies suggest that CB units contain 25–50-fold fewer early engrafting neutrophil and platelet progenitor cells than mobilized peripheral blood and that the frequency of these progenitors in individual CB grafts is independently variable and correlates with the clonogenic CFU-GM and CFU-Mk content, respectively (Cheung *et al.*, 2012). Indeed, CB grafts with a higher content of CFU and viable $CD34^+$ cells ($>1.8 \times 10^5$ $CD34^+$ cells transplanted per kilogram of the recipient's body weight) demonstrate improved median time to and probability of neutrophil and platelet engraftment (Avery *et al.*, 2011; Lemarie *et al.*, 2007; Migliaccio *et al.*, 2000; Page *et al.*, 2011; Scaradavou *et al.*, 2010; Wagner *et al.*, 2002). The latter, as well as longer term hematological reconstitution of CB $CD133^+CD34^+$ HSC/HPC post-transplant (Cheung *et al.*, 2013; Drake *et al.*, 2011) can be measured in the peripheral blood in surrogate NSG mouse models (Cheung *et al.*, 2012; van der Garde *et al.*, 2014), although neutrophil recovery is over 10-fold lower in peripheral blood than bone marrow in NSG recipients (Cheung *et al.*, 2012). However, longer term and serial transplantation in NSG mice (Cheung *et al.*, 2013; Drake *et al.*, 2011) and especially transplantation into non-human primates more closely resembles the human *in vivo* transplant setting (Kim *et al.*, 2014; Watts *et al.*, 2013; Wu *et al.*, 2014). Recent studies have demonstrated that ~half of the mobilized peripheral blood $CD34^+$ HSC/HPC contribute to 3–10-year long-term and ~half to short-term repopulation, while 4–10% of clones (or ~0.1% of $CD34^+$ cells) have durable lympho-myeloid reconstitution in non-human primates (Kim *et al.*, 2014). The limited number of HSCs in a single CB unit often restricts these grafts to children and small adults. Although double CB units can be transplanted into adults to enhance stem cell content, this does not significantly improve early neutrophil and platelet recovery post-transplant and only one of the transplanted CB units generally engrafts long term (Scaradavou *et al.*, 2013).

The numbers of HSC/HPCs in a CB graft can be increased by culturing human CB $CD34^+$ or $CD133^+$ HSC/HPC *ex vivo* in the presence of cytokines and small molecules prior to transplantation. Notably, the $CD133^+$ fraction of human CB has been shown to contain all repopulating cells, at least in surrogate models of hematopoiesis (Takahashi *et al.*, 2014). Clinical trials have shown that *ex vivo* CB HSC/HPC expansion can improve the outcome of CB transplantation in terms of time to neutrophil engraftment (Danby and Rocha, 2014; Delaney *et al.*, 2013). However, experimentally, *ex vivo* culture can also deplete, expand or maintain the long term engrafting HSCs in a CB graft (Fares *et al.*, 2014; Gu *et al.*, 2014). The protocol for expanding CB cells should therefore not only focus on the highest fold expansion of the early engrafting neutrophil and platelet progenitor cells but also on maintaining and amplifying the durable long term repopulating HSC.

The rationale behind the use of cytokines and small molecules to expand such cells is based on knowledge of the cues that signal to HSC/HPC cells from their microenvironmental niches in the bone marrow (Mendelson and Frenette, 2014; Morrison and Scadden, 2014). The efficiency of the *ex vivo* expansion of HSC/HPC subsets thus depends on the cytokine and small molecule combinations used and can be further modulated with 3D scaffolds or by controlling the supply of nutrients and depletion of inhibitory molecules in the cultures (Csaszar *et al.*, 2012, 2014; Pepperell and Watt, 2013). In most clinical protocols, a minimum basic combination of stem cell factor (SCF), thrombopoietin (TPO) and Flt3-ligand (Flt3L) is used (Pepperell and Watt 2013; Piacibello *et al.*, 1997). Addition of other cytokines such as interleukin-6 (IL-6), hyper-IL-6, interleukin-3, G-CSF, insulin growth factor binding protein 2 (IGFBP-2), Notch ligands and Angiopoietin-like 5 (Angptl5) can improve the fold expansion of the human $CD34^+$ and/or $CD133^+$ HSC/HPC (Benveniste *et al.*, 2014; Dahlberg *et al.*, 2014; Pepperell and Watt, 2013; Rappold *et al.*, 1999; Tarasova *et al.*, 2011; Zhang *et al.*, 2008). More recently, with the ability to segregate human HSC/HPC into phenotypically enriched cell subsets (Goergens *et al.*, 2013; Notta *et al.*, 2011) and to correlate this with their transplantability into surrogate models, other factors [e.g. the aryl hydrocarbon receptor antagonist SR1, HDAC and apoptotic inhibitors, pyrimidazoindole derivatives (histone demethylases), dmPGE2, nicotinamide] have been added to basic cytokine cocktails (e.g. SCF, TPO, Flt3L ± other factors) to enhance the content of short or long term repopulating HSC/HPC (Boitano *et al.*, 2010; Chaurasia *et al.*, 2014; Fares *et al.*, 2014; Fonseca-Pereira *et al.*, 2014; Hagedorn *et al.*, 2014; Horwitz *et al.*, 2014; Pepperell and Watt, 2013). For clinical application, GMP-grade expansion of $CD133^+$ or $CD34^+$ HSC/HPC is required but is a costly procedure and addition of multiple cytokines increases the cost of an expanded product. Therefore, it is vital to use a basic cytokine combination that provides the best expansion without increasing the cost of the procedure while preserving stemness characteristics.

In this study, we have analyzed the influence of different combinations of the cytokines SCF, TPO, Flt3L, IGFBP-2, Angptl5, IL-6, fibroblast growth factor-1 (FGF-1) and Oncostatin M (OSM) on the fold expansion of human CB $CD133^+CD34^+$ cells, which contain HSCs and their multipotent (MMP, LMPP, MLP and GMP) progeny (Goergens *et al.*, 2013). We present a computational approach to elicit the effect of different cytokines, by modeling the signaling cascades of the cytokines and thereby their effect on the proliferation, differentiation and survival of these cells in *ex vivo* culture. We retrieved signaling pathways of the specified cytokines from specialized literature and by database mining. Then, we extracted in a rational way all the prevalent effects of signals, merging them into an integrated graph (see Supplementary Fig. S1) that we used to model, by means of ordinary differential equations (ODEs), the biological microenvironment. The model is intrinsically multiscale, i.e. it takes into account events at the molecular level (biochemical signaling pathways) and at the cellular level (differentiation, survival and duplication of target $CD34^+CD133^+$ cells and the dynamics of cytokines used in the cocktail). The model was tuned by reference to *in vitro* experiments and then used as a virtual lab. The virtual lab was then applied to search for cytokine cocktails that maximize the duplication of and minimize the loss of $CD34^+$ and $CD133^+$ cells, using a trial and error procedure. The best *in silico* protocol was then confirmed by *in vitro* experiments. This study provides evidence that *in vitro* data relating to the proliferation of human HSC/HPC can be theoretically modeled with a computational approach. In future applications, this model could be extended to

study whether other cytokines and/or small molecules can improve the survival, proliferation and/or differentiation of defined HSC/HPC subsets or other stem cells (e.g. mesenchymal stem cells) that are used in cellular therapy or inhibit the proliferation of cancer initiating or stem-like cells.

2 Materials and methods

2.1 CB collection and isolation of the CD133$^+$ cells

Human CB units were collected with written informed pre-consent and ethical approval from Oxford and Berkshire National Research Ethical Committees and studies conducted with approval of the NHSBT research committee. Mononuclear cells (MNC) were isolated by density gradient centrifugation on lymphocyte separation medium 1077 (PAA Laboratories, Pasching, Austria; density < 1.077 g/ml). CD133$^+$ cells were isolated from the MNC with immunomagnetic beads (Miltenyi Biotec, Bergisch Gladbach, Germany). After isolation, the cells were cryopreserved in 10% DMSO in FCS and stored at -150°C. Cells were analyzed for the purity of the isolation with flow cytometry on a BD LSR II (BD Biosciences, CA) using CD34-APC, CD133-PE and the appropriate isotype controls (all Miltenyi Biotec). The raw data used for the analysis and the appropriate flow cytometry data along with an appropriate MIFlowCyt description (Lee *et al.*, 2008) are supplied in Supplementary Table S4 and Document 2.

2.2 *In vitro* expansion of CD133$^+$ cells

CD133$^+$ cells were thawed and resuspended in serum-free Stemspan SFEM medium (Stemcell Technologies, Vancouver, Canada). Cells were allowed to recover from cryopreservation by incubating overnight at 37°C with 5% CO_2 in 24-well tissue culture plates at 1×10^5 cells/well containing Stemspan SFEM and 100 ng/ml SCF, 100 ng/ml IL-6, 100 ng/ml Flt3L and 20 ng/ml TPO (all CGS, Cambridge, UK). After overnight culture, the cells were harvested, washed to remove all cytokines and resuspended in Stemspan SFEM. Cells were then loaded into NANEX nanofiber plates (Arteriocyte, MA) at 1×10^3 cells/ml (Pepperell and Watt 2013) with a single cytokine or various combinations of the following cytokines: SCF 100 ng/ml, IL-6 100 ng/ml, Flt3L 100 ng/ml, TPO 20 ng/ml, FGF-1 10 ng/ml (all CGS), OSM 50 ng/ml, Angptl-5 100 ng/ml (both Miltenyi Biotec) and/or IGFBP-2 100 ng/ml (Preprotech, London, UK) and incubated at 37°C in 5% CO_2 for 8 days. Cells were analyzed for viable CD34 and CD133 expression by flow cytometry (Pepperell and Watt, 2013). After 8 days of culture, the cells were harvested from the plates and the volume of the cell suspension determined. The cells were again analyzed for the expression of CD34 and CD133 by flow cytometry, and the concentration of the cells was determined using countbright beads (Life Technologies, Paisley, UK) to calculate the number of cells after expansion. The fold expansion of the total nucleated cells (TNCs) was calculated by dividing the total number of cells harvested after expansion with the number of input cells. By multiplying the fold TNC expansion by the percentage of CD133$^+$CD34$^+$ cells post-expansion and comparing this to the input cells, we calculated the fold expansion of the CD133$^+$CD34$^+$ cells.

2.3 Computational modeling of the cytokine effects on the CD133$^+$ cell population

The first step in realizing any tractable model that is able to represent a biological problem is to analyze the problem itself, trying to catch the most prominent features and leaving out secondary and less important features.

There are several examples in literature that apply this important approach (Camporeale *et al.*, 2003; Castiglione *et al.*, 2012; Chiacchio *et al.*, 2014; Germain *et al.*, 2011; Pappalardo *et al.*, 2014a, b). In this study, many cocktails of combined cytokines are used with the goal of maximizing CD133$^+$ cell fold expansion by culturing the CB cells *ex vivo*. It is therefore clear that, to model the entire biological scenario, we need to take into account two processes that happen on different scales: the *population level,* which describes CD133$^+$ cell behavior, including duplication and differentiation, and the *intracellular* level, which takes into account all the important biochemical pathways that are triggered by the use of cytokines and determine the behavior of cells at the population level. These two levels must be reproduced and connected to describe exhaustively the biological problem. The biochemical pathways are cell dependent, in the sense that two different cells may internally follow different pathways, and this would entail as many simulations at the intracellular level as the number of involved cells at the population level. It is clear that different cocktails may lead to very variable results on the basis of the biochemical pathways that are triggered. Hence, for all the cytokines analyzed, the most important signal transduction pathways have been gathered from literature.

An exhaustive model of a single biological pathway already entails very complex models based on systems of tens to thousands of ODEs or complex Petri Nets (the solution for which is in any case usually carried out by ODE systems). Moreover, in many cases, it includes unknowns that cannot be measured experimentally (Tarasova *et al.*, 2011). The complexity grows if we consider that a single cytokine usually triggers more than one pathway. Thus, it is clear that the realization of a model which accurately describes, combines and aggregates all the pathways involved with the use of a cocktail of cytokines is not viable, at least initially. We instead tried to catch and reassume the final effects of the pathways activated by cytokines on the CD133$^+$ cell population. To this end, we initially identified and labeled all the pathways that involved the use of the identified cytokines, clustering all similar pathways (with the same effects) as one; at the same time, we determined from literature the main effects of any pathway cluster by examining three possible principal effects on the CD133$^+$ cell population: *survival*, *duplication* and *differentiation*. Survival refers to the ability of a pathway to stimulate all the processes that involve an increase of cell survival, such as *cytoskeleton reinforcement*; duplication refers to the capability of stimulating cells to duplicate by maintaining CD133 positivity and differentiation considers all the pathways that stimulate maturation of CD133$^+$ cells into those cells where CD133 expression is lost and CD34 expression is retained and then both CD133 and CD34 expression is subsequently lost (see Supplementary Table S1).

These three effects represent the connection point between the intracellular and population models. The intracellular model is used to determine the survival, duplication and differentiation coefficients associated with the use of a given cocktail of cytokines. Such coefficients are then used as parameters for the population model and will influence survival, duplication and differentiation rates of involved populations (see Supplementary Fig. S1). The weight of every pathway cluster on one or more of the coefficients is estimated on the basis of multiple *in vivo* experiments that have been carried out with different cytokines cocktails.

For analysis at the population level, we started by taking into account two populations: *CD133$^+$CD34$^+$ cells* and their

$CD133^{-}CD34^{+}$ or $CD133^{-}CD34^{-}$ *differentiated progeny*. The first population takes into account all the cells that have not lost CD133 and CD34 expression, whereas the second one takes into account all the cells that differentiated and thus lost CD133 expression. Both the populations composed of two sub-populations, normal and activated. Normal cells represent cells that interact with cytokines. Triggered or activated cells can then *survive*, *duplicate* or *differentiate* in accordance with the effects activated by cytokine-induced pathways. After that, the cells revert to their normal or non-activated state and become prone to interact again with cytokines that can stimulate further activation. In Supplementary Figure S1, we show the complete conceptual model for both intracellular and population models.

2.4 Formal description of the ODE model

The key aspect of the modeling approach we present is given by the connection of two models at different levels, namely, an intracellular model and a cellular population model. This connection is achieved by using probabilities and/or rates that are estimated by the intracellular-model and then cellular behavior is determined at a higher level within the population model. Such an approach can in principle be employed using any kind of modeling techniques suitable for modeling at the intracellular and population levels. Choosing the right modeling techniques is fundamental as it mainly depends on the complexity of the biological problem we are dealing with. It should be noted that the use of different modeling techniques requires a technique that allows the communication between the two models.

In building up our multi-scale model, we first analyzed how to build the signaling pathway model. To this end, we used a two-step 'qualitative–quantitative' procedure: in the first step ('qualitative'), we established which cytokine-induced pathways are fundamental for the effects being analyzed (*duplication*, *differentiation* and *survival*). We used the data from literature presented in Section 2.5 and from public databases such as Pathway Commons network (http://www.pathwaycommons.org) and KEGG (Kyoto encyclopedia of genes and genomes). This first step allowed us to determine which pathways needed to be taken into account and represented in the model. We then developed a conceptual scheme (see Supplementary Fig. S1) that not only summarizes all the information we gathered from literature and databases for creating the pathway model, but it also includes the cellular conceptual model and the connection points between the two levels (the duplication, differentiation and survival rates). We used ODEs for both the models because the model at population level was not so complex. This allowed us to use only one modeling technique and the same software for both the models, avoiding the need to find a more complex way for the two models to communicate. In particular, we used Berkeley Madonna for the simulation of the ODE system. To run the model, one has to download the latest version of Berkeley Madonna (http://www.berkeleymadonna.com/jmadonna/jmadrelease.html) and then download the source code of the model as indicated in the availability section (http://www.francescopappalardo.net/Bioinformatics_CD133_Model).

In the second step ('quantitative'), we determined the weighting for the pathways over the rates that are used in the population model. In this case, we mainly used data directly coming from *in vitro* experiments using one cytokine at a time. *In vitro* experiments with the combined use of two or three cytokines were then used to establish the presence of interrelations among cytokines and their weighting. Finally, tuning with free parameters was achieved using a trial and error procedure in such a way that the model was completely able to reproduce all experiments with one, two or three cytokine combinations. Adding a new cytokine to the model required us to follow the procedure already presented, taking into account both qualitative and quantitative steps. The first equations we present relate to cytokine behaviors. Cytokines are added at the beginning of the experiment. They interact with cognate receptors on normal cells (both $CD133^{+}$ and $CD34^{+}$ HSC/HPC and $CD133^{-}$ differentiated cells) and can disappear from the system due to natural degradation pathways. So the typical equation structure is given by the following equation:

$$\frac{dC_i}{dt} = -m_i C_i - x_i(S + D)C_i$$

where C_i represents the i_{th} cytokine, m_i is the degradation rate, x_i is the absorbing or interacting rate and S and D represent the normal $CD133^{+}$ and differentiated cell populations, respectively.

As already stated, we take into account four populations altogether: normal inactivated $CD133^{+}$ cells (S), normal differentiating cells (D), duplicating $CD133^{+}$ cells (S_a) and duplicating $CD133^{-}$ differentiating cell subsets (D_a). These populations are described by the following system of ODE:

$$\begin{cases} \dfrac{dS}{dt} = -(m_1 - \text{sur}) \cdot S - k_1 S + k_2 S_a \\ \dfrac{dS_a}{dt} = -(m_1 - \text{sur}) \cdot S_a - \text{dif} \cdot S_a + \text{dup} \cdot S_a + k_1 S - k_2 S_a \\ \dfrac{dD}{dt} = -(m_2 - \text{sur}) \cdot D - k_3 D + k_4 D_a + \text{dif} \cdot S_a \\ \dfrac{dD_a}{dt} = -(m_2 - \text{sur}) \cdot D_a + \text{dup} \cdot D_a + k_3 D - k_4 D_a \end{cases}$$

We have made the assumption that both normal (S and D) and duplicating (S_a and D_a) cell populations behave in a similar way. Normal $CD133^{+}$ cells (S) have a non-zero value at the beginning of the experiment. They can disappear from the system through apoptosis (m_1 coefficient), although this programmed death rate can be lowered thanks to the added cytokines, which can activate intracellular signaling pathways that improve survival (-sur coefficient). Then such cells, after interacting with a specific growth factor, can activate a signaling pathway resulting in the duplication of the cell population (S_a) with a given rate k_1 and (once they duplicate) they revert to an inactivated state with a given rate k_2. Duplicating $CD133^{+}$ cells (S_a) are assumed to have the same death coefficient as normal inactivated $CD133^{+}$ cells *(-(m_1-sur))* and can duplicate again or proceed to differentiate with dup and dif coefficients, respectively. Such coefficients are estimated on the basis of the cytokine-induced pathways at intracellular level. Since their number is 0 at the beginning of the experiment, the only source term for S_a cells is given by the term $k_1 S$, which indicates activation from the normal $CD133^{+}$ inactivated state. Finally, they can go back to the normal inactivated state with a given coefficient k_2. Normal differentiated cells (D) can be introduced into the system due to cytokine effects that stimulate $CD133^{+}$ cells to differentiate ($+\text{dif}S_a$). Such cells have a similar death coefficient as described before, can be activated allowing their differentiation ($-k_3 D$) and can revert to an inactivated state ($+k_4 D$). Finally, duplicating differentiating cells (D_a) are introduced into the system from the D population ($+k_3 D$), can go back to the D subpopulation ($-k_4 D$), can duplicate with a coefficient estimated on the basis of cytokine-induced pathways ($+\text{dup}D_a$) and can be exposed to programmed cell death as previously described *(-(m_2-sur))*. The equations at the intracellular level describe the activation of intracellular pathways induced by

cytokines administered at the cellular level. The activation of a given pathway P can be due to the administration of a given Cytokine. However, when two or more cytokines are administered, one should take into account not only singular effects over the pathway but also the combined effects that can positively and/or negatively influence the pathway itself. It is clear that the effect of a cocktail of two cytokines cannot be represented only by the sum of the effects obtained by administering such cytokines one at a time since competition, inhibition or synergistic mechanisms may arise. In particular when we use three cytokines, we should take into account the singular effects of the cytokines, the effects given by all the combinations of three cytokines grouped by two and the combined effect of all three cytokines. So in general, we can describe the activation of a pathway by a cocktail of cytokines using the following equation:

$$\frac{dP}{dt} = -\mu_P P + \sum_{i\in I_P} A_i f_1(C_i) + \sum_{i,j\in I_P} A_{ij} f_2(C_i, C_j) + \sum_{i,j,k\in I_P;} A_{ijk} f_3(C_i, C_j, C_k) + \ldots + A_{1\ldots n} f_n(C_1 \ldots C_n) \quad (1)$$

Where P_h is the h^{th} pathway, $-\mu_p P_h$ describes the loss of activation of the pathway P_h, A_i is a vector of coefficients which describe the effects of cytokine C_i over the pathway, A_{ij} is a 2D symmetric matrix (with $A_{ii}=0$) that contains the coefficients of the effects of the combined administration of two cytokines C_i and C_j; A_{ijk} is a 3D symmetric matrix (with $A_{ijk}=0$ if $i=j$, $j=k$ or $k=i$) that contains the coefficients of the effects of the combined administration of three cytokines C_i, C_j and C_k; $A_{1\ldots n}$ is the coefficient that describes the combined administration of all cytokines and

$$f_j(C_1, C_2, ..., C_j) = \sqrt[j]{C_1 \cdot C_2 \cdot .. \cdot C_j}$$

is a set of n normalized functions that is used to describe the simultaneous presence of two or more cytokines. The signaling pathway equations are then used to estimate the three coefficients (sur for survival, dif for differentiation and dup for duplication) that determine the effects of the pathways at the cellular level. The three coefficients are estimated at every time-point using the following equations:

$$\begin{cases} \text{sur} = G_1\left(\sum_{i=1}^{n} \alpha_i P_i\right) \\ \text{dup} = G_2\left(\sum_{i=1}^{n} \beta_i P_i\right) \\ \text{dif} = G_3\left(\sum_{i=1}^{n} \gamma_i P_i\right); \\ \text{with} \\ G_j(x) = \dfrac{x^{Hj}}{x^{Hj} + c_j}, j = 1, 2, 3 \end{cases} \quad (2)$$

where n is the total number of pathways; P_i represents the i_{th} pathway; α_i, β_i and γ_i are coefficients set equal to 1 if the pathway P_i influences survival, duplication and/or differentiation, 0 elsewhere (see Supplementary Table S1); G_j ($j=1..3$) is a set of bounded functions that is used to model the fact that all cells are subject to biological constraints, no matter how many external stimuli are provided (i.e. a cell cannot duplicate over a certain ratio even if cytokine dosage is increased more and more); Hj and cj are tuned constants.

2.5 Data and biology driven tuning of the ODE model

To reproduce the *in vitro* experiments in our model, it is important to determine both the singular and combined effects of the cytokines on the activation of signal-transduction pathways. These effects will influence the value of the coefficients defined inside the interaction matrices A. It is clear that not all the coefficients will have a non-zero value, and consequently, many terms inside the equations that describe activation pathways can be omitted. It is worth mentioning that the signaling transduction analysis and clustering procedure we have already described have allowed us to qualitatively, but not quantitatively, establish the influence of cytokines over activation pathways. Hence, the values of the coefficients inside the A_i vector have been set by simulating the administration of one cytokine at a time in such a way that *in silico* results are comparable with *in vitro* results. Then, we proceeded by determining the coefficients of the A_{ij} matrix by administering two cytokines at a time and comparing again *in silico* with *in vitro* results. In many cases, the presence of enhancing or suppressing effects of these coefficients was confirmed by several *in vitro* experimental studies, in particular: (i) the addition of IL-6 to SCF, TPO and Flt3L supported $CD34^+/CD133^+$ cell expansion (Pepperell and Watt, 2013; Rappold *et al.*, 1999); (ii) combination of TPO with another early acting cytokine would support expansion of repopulating cells in immunodeficient mice (Piacibello *et al.*, 1997); (iii) the association of Flt3L and TPO may entail a progressive, steady increase in cell production (Piacibello *et al.*, 1997); (iv)Flt3L may synergize well with a number of other hematopoietic growth factors and increase the response of HSC/HPC to other growth factors. The synergistic effect in combination with IL-6, SCF and TPO has been demonstrated (Haylock *et al.*, 1997; Koller *et al.*, 1996; Ohmizono *et al.*, 1997; Shurin *et al.*, 1998); (v) TPO alone may induce differentiation of $CD34^+$ cells into $CD41^+$ cells, with limited total leukocyte expansion, but the addition of SCF to TPO can decrease significantly the percentage of CB $CD41^+$ cells (De Bruyn *et al.*, 2005; van der Garde *et al.*, 2014); (vi) FGF-1 can hamper HSC/HPC differentiation into more mature hematopoietic cells (De Haan *et al.*, 2003; Faloon *et al.*, 2000); (vii) OSM cooperates with SCF to enhance CB $CD133^+CD34^+$ proliferation and counteracts the SCF-mediated loss of repopulating cells in immunodeficient mice (Oostendorp *et al.*, 2008); (viii) angptL5 and IGFBP2 could enhance $CD133^+CD34^+$ HSC/HPC expansion and differentiation (Drake *et al.*, 2011; Zhang *et al.*, 2008). To this end, all the experimental data coming both from literature and from the *in vitro* data for 1, 2 and 3 or more cytokine combinations were used to tune the model. Other PMIDs of articles that describe the pathways we used in the analyses are provided in Supplementary Table S5. The final intracellular model (Supplementary Fig. S2), the variables' definition (Supplementary Table S2) and the values of the coefficients (Supplementary Table S3) are presented as Supplementary Document 1.

3 Results and discussion

Many clinical and experimental protocols for expanding CB $CD34^+$ or $CD133^+$ HSPCs include a basic cytokine cocktail of SCF, TPO, Flt3L and IL-6 and then additional factors are added to enhance HSC/HPC expansion. As the basis for developing our model, we first examined the effects of these four cytokines on the expansion and differentiation of purified CB $CD133^+$ HSC/HPCs in our 8-day serum-free 3D scaffold culture system, without or with the addition of AngptL5, IGFBP2, OSM and FGF-1. The results of these analyses for four different CB donors are shown in Figure 1. Notably, the addition of AngptL5 and IGFBP2 enhanced the mean TNC and $CD133^+CD34^+$ cell fold expansion, and this was further enhanced by addition of OSM and FGF-1. It should be noted that SCF has

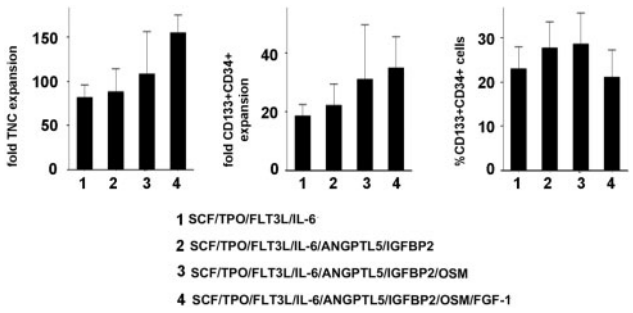

Fig. 1. Culture of CB CD133$^+$ for 8 days on 3D nanofiber scaffolds under serum-free conditions with four different cytokine combinations. Results presented after the 8-day culture are: (left) fold TNC expansion calculated by dividing the number of nucleated cells harvested after expansion by the number of nucleated cells added at the start of the culture; (middle) fold CD133$^+$CD34$^+$ expansion calculated by multiplying the fold TNC expansion by the percentage of CD133$^+$CD34$^+$ determined by flow cytometry after expansion; (right) percentage of CD133$^+$CD34$^+$ cells analyzed by flow cytometry using the appropriate isotype controls to distinguish positive from negative cells. Values are mean ± SEM from $n = 4$ individual CB donor analyses

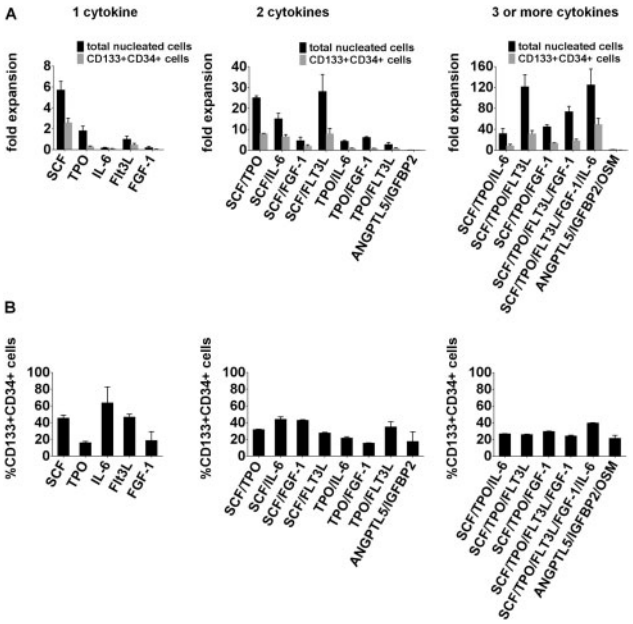

Fig. 2. Culture of CB CD133$^+$ for 8 days on 3D nanofiber scaffolds under serum-free conditions with individual or two or more different cytokine combinations. Results presented after the 8-day culture are as follows. (**A**) Fold TNC and CD133$^+$CD34$^+$ expansion. (**B**) Percentage of CD133$^+$CD34$^+$ cells analyzed by flow cytometry using the appropriate isotype controls to distinguish positive from negative cells. Values are mean ± SEM from $n = 3$ individual experiments using pooled CB donor cells

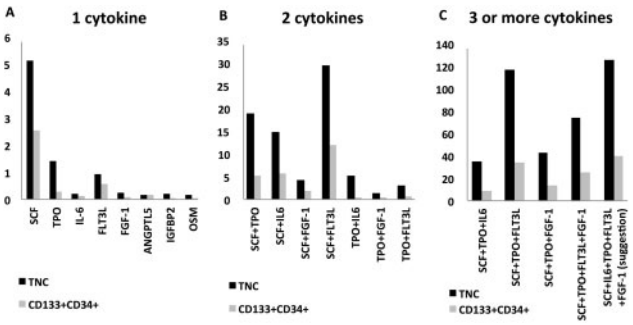

Fig. 3. *In silico* results. (**A**) *In silico* results showing the effects of adding one cytokine at a time. Compared with the other cytokines, SCF alone markedly improves both TNC and CD133$^+$CD34$^+$ fold expansion. (**B**) *In silico* results showing the effects of adding two cytokines to the cocktail added to CD133$^+$ cell cultures. Once again, SCF plays a fundamental role in both TNC and CD133$^+$CD34$^+$ fold expansion. (**C**) *In silico* results showing the effects of some cocktails composed by three or more cytokines on the CD133$^+$ cells. As observed *in vitro*, the model shows that SCF and TPO represent an important starting point for the formulation of any optimal cocktail. The introduction of FGF-1 to the SCF+TPO+Flt3L cocktail seems to worsen the overall expansion results for both TNC and CD133+CD34+ cells. However, the three cytokine combination of SCF+TPO+Flt3L with the addition of IL-6 and FGF-1 appears to be a better possible candidate than SCF+TPO_Flt3L for optimal cell expansion within the limitation of these studies. These cocktails also preserve an acceptable level of CD133$^+$CD34$^+$ cells

been reported to promote HSC expansion by synergizing with such factors as TPO, Flt3L and cytokines, which signal via the gp130 receptor or IL-6, OSM and IL-11 (see Oostendorp *et al*., 2008 and references therein). Indeed, OSM has been demonstrated to be particularly important in modulating SCF-induced ERK activation in human CB CD133$^+$CD34$^+$ cells, increasing their proliferation while preserving their *in vivo* repopulating ability (Oostendorp *et al*., 2008). We next added or subtracted cytokines to/from the basic SCF, TPO, Flt3L and IL-6 cocktail. Figure 2 shows the mean fold expansion of TNC and CD133$^+$CD34$^+$ cells (Fig. 2A) and the percentage of the CD34$^+$CD133$^+$ cells after expansion (Fig. 2B) for 19 of the individual cytokines or cytokine combinations tested.

Some of these cocktails were used for the development and the tuning of the model, while some of them were employed to validate the predictions that the model made. In general, addition of a single cytokine did not result in expansion of CB cells from the enriched CD133$^+$ starting population over 8 days on our 3D nanofiber scaffold under serum-free culture conditions, with the exception of SCF and TPO (5.7 ± 0.9 and 1.8 ± 0.5-fold expansion of TNC, respectively). However, only SCF was able to expand cells with the double CD133$^+$CD34$^+$ phenotype (SCF: 2.6 ± 0.4-fold, TPO: 0.3 ± 0.1-fold). This is consistent with SCF possessing weak proliferative activity when used alone (Tarasova *et al*., 2011). We used these experimental data to start tuning the model. FLt3L alone in the cultures resulted in the same TNC number after expansion as before expansion (1.0 ± 0.3-fold expansion), but half of these cells had lost their double positive phenotype (fold CD133$^+$CD34$^+$ expansion: 0.5 ± 0.2). Less than 20% of the cells survived after when IL-6, FGF-1 or Oncostatin-M (OSM) were added as the sole cytokine (Fig. 2 and data not shown). This indicates that SCF is essential for the survival of these cells and that this factor cannot be excluded from the cytokine cocktail that is added to the culture medium. TPO alone doubled the number of TNC, but the proportion of CD133$^+$CD34$^+$ cells was reduced to only a third of the starting population, suggesting that TPO can provide a survival signal but can also promote differentiation into more mature phenotypes. This is in agreement with our recent demonstration that TPO can enhance early platelet engraftment and hence can enhance platelet progenitor cell differentiation at the expense of maintaining longer term repopulating cells (van der Garde *et al*., 2014). We used our *in vitro* results that Flt3L better maintains CD133+CD34+ cell content than TPO, IL-6 and FGF-1 (Fig. 2) and reports in the literature (Shurin *et al*., 1998) that the RAF/MEK/ERK pathway is triggered when Flt3L is added to cells. Figure 3A depicts *in silico* results of the model simulating the addition of one cytokine at a time on the fold expansion of TNC and CD133$^+$CD34$^+$ cells and also shows that

Flt3L promotes a better $CD133^+CD34^+$ fold expansion when compared with the other cytokines, excepting for SCF that has a stronger effect. For this and other cytokines tested *in vitro* (Fig. 2 and data not shown), the model was able to reproduce the *in vitro* results (Fig. 3A). Furthermore, the *in silico* results also highlight the importance of SCF for both cell populations. Adding a second cytokine to either SCF or TPO markedly improved the TNC and $CD133^+CD34^+$ cell expansion. Addition of TPO, IL-6 or Flt3L to SCF resulted in 25.1 ± 1.0, 15.0 ± 2.7 and 28.1 ± 8.3-fold TNC expansion and 7.9 ± 0.2, 6.5 ± 1.0 and 7.9 ± 2.6-fold expansion of the $CD133^+CD34^+$ cells, respectively (Fig. 2). This is consistent with the demonstration that these four cytokines are early acting factors which act synergistically on HSC/HPC (Tarasova *et al.*, 2011). FGF-1 added to SCF (4.6 ± 1.8-fold TNC and 2.0 ± 0.7-fold $CD133^+CD34^+$ expansion) did not improve expansion as much as SCF alone (Fig. 2). Addition of IL-6, FGF-1 or Flt3L to TPO improved expansion of TNC only (2.7–6.1-fold) but to a lesser extent than when each of these factors was added to SCF. This again shows that SCF is an essential component of the culture medium. These data were also used to tune the *in silico* model. In particular, Figure 3B shows the *in silico* results after the application of the model to simulate the effects on TNC and $CD133^+CD34^+$ cells when two cytokines were added. The model correctly reproduced the *in vitro* experiments obtained when SCF or TPO were used in combination with another cytokine. Similar results were also reported in Piacibello *et al.* (1997).

Adding three cytokines to the culture medium further improves expansion but only if both SCF and TPO are present in the cytokine cocktail. Figure 2 demonstrates that the expansion improves when IL-6, FGF-1 or Flt3L is added to SCF and TPO (25.5 ± 5.8-fold TNC and 7.9 ± 0.2-fold $CD133^+CD34^+$ expansion for SCF and TPO and 31.3 ± 10.1, 44.5 ± 4.1, 120.9 ± 23.3-fold TNC and 8.4 ± 2.8, 13.1 ± 1.0 and 31.2 ± 6.4-fold $CD133^+CD34^+$ expansion with IL-6, FGF-1 or Flt3L addition, respectively). The expansion seen after the addition of FGF-1 to SCF and TPO was thus 3-fold lower compared with the addition of Flt3L to SCF and TPO, while adding Flt3L to SCF and TPO led to the highest fold expansions of both TNC and $CD34^+CD133^+$ cells (Fig. 2). Thus, combining these factors, which when used alone can maintain or expand limited numbers of cells, leads to a synergistic effect that dramatically improves the expansion capacity of the cells. The addition of AngptL5, IGFBP2 or OSM alone with SCF and TPO did not improve the expansion over 8 days compared with the combination of SCF and TPO (25.5 ± 5.8-fold TNC and 7.9 ± 0.2-fold $CD133^+CD34^+$ expansion for SCF and TPO and 14.6 ± 4.5, $4.1 + 8.5$, $11.1 + 3.1$-fold TNC and 6.6 ± 2.5, $1.6 + 0.7$ and 4.1 ± 1.3-fold $CD133^+CD34^+$ expansion with IL-6, FGF-1 or Flt3L addition, respectively).

The *in vitro* results based on the combination of SCF/TPO with one other cytokine, namely IL-6, FGF1 or Flt3L were also used to tune the *in silico* model (Fig. 3C). We then used the model to see if a better cocktail than SCF/TPO/FLT3L was achievable. Simulations showed that the addition of FGF-1 to the SCF/TPO/Flt3L cocktail worsened both TNC and $CD133^+CD34^+$ fold expansion, suggesting the presence of one or more inhibition/competition mechanisms between FGF-1 and the other used cytokines. We then added IL-6 to the SCF/TPO/FGF-1/Flt3L cocktail, to try to forecast the combined effect of SCF/TPO/IL-6/FGF-1/Flt3L on $CD133^+$ cell expansion since *in silico* results suggested that such an addition may generate marginally higher absolute numbers of both TNC and $CD133^+CD34^+$ cells compared with the SCF/TPO/Flt3L cocktail, and this therefore needed to be verified *in vitro*. In the *in vitro* experiments, SCF/TPO/Flt3L/FGF-1/IL-6 did indeed prove better for TNC (124.5 ± 30.9-fold) and $CD133^+CD34^+$ (49.0 ± 11.8-fold) expansion than SCF/TPO/Flt3L (Fig. 2). Adding IL-6 to SCF, TPO and Flt3L without FGF-1 also enhanced TNC expansion but was on average less potent than the five cytokine combination for $CD133^+CD34^+$ cell expansion (136.4 ± 15.6 and 45.4 ± 5.6-fold, respectively, with SCF/TPO/Flt3L/IL-6). It is worth noting that some cytokine interrelations have not been taken into account due to the lack of experimental data, or because some of them are not known, disputed or not clear. As far as new data are concerned, these can be added to the model when available to better forecast the combined effects of missing cytokine cocktails.

As mentioned in Section 1, the preservation of an immature progenitor phenotype (i.e. maintaining the expression of $CD133^+CD34^+$ cells), while promoting their differentiation into $CD34^+CD133^-$ cells, is an important aspect of expansion. This was indeed the main target of the *in silico* model. The percentage of $CD133^+CD34^+$ cells after expansion on a 3D scaffold in serum-free medium for 8 days is shown in Figures 1 and 2. The supply of a scaffold is often absent in other expansion protocols and this can lead to longer culture periods. Addition of a single cytokine in our culture system showed that SCF maintains the double positive phenotype better than TPO alone ($45.4 \pm 3.8\%$ versus $15.9 \pm 1.8\%$). This is also reflected by the low expansion of $CD133^+CD34^+$ cells by TPO. Addition of other cytokines such as IL-6 or Flt3L alone resulted in higher percentages of $CD133^+CD34^+$ cells, but since there was no net fold TNC expansion, these results are difficult to interpret since it is more likely that these high percentages show that some $CD133^+CD34^+$ cells survive better with these added cytokines. Addition of Flt3L to medium containing SCF resulted in lower percentages of double-positive cells ($27.6 \pm 0.9\%$) than addition of IL-6 ($44.0 \pm 3.0\%$), TPO (31.6 ± 0.7) or FGF-1 ($42.8 \pm 0.8\%$), with SCF, but, due to the larger increase in TNC expansion, the fold expansion of the $CD133^+CD34^+$ cells was higher nonetheless. One possibility is that Flt3L is able to stimulate proliferation of the $CD133^+CD34^+$ cells as well as enhance the asymmetrical division of these cells into more differentiated cells. Adding Flt3L to both TPO and SCF yielded a higher fold TNC expansion, but a lower percentage of $CD133^+CD34^+$ cells ($25.7 \pm 0.7\%$), when compared with addition of IL-6 ($26.6 \pm 0.4\%$) or FGF-1 ($29.5 \pm 0.6\%$). Thus, our model would predict a minimum of three cytokines (SCF/TPO/Flt3L) as the basic starting conditions for further cytokine and small molecule additions in terms of CB $CD133^+CD34^+$ expansions.

4 Conclusions

In this article, we have examined the effects of eight cytokines on the expansion of CB $CD133^+CD34^+$ cells and their differentiation into $CD133^-CD34^-$ cells using an 8-day 3D scaffold serum-free culture system. These cytokines are used experimentally or in clinical studies of CB HSC/HPC expansion to enhance HSC numbers and prevent delays in early hematological engraftment. As was expected, our experimental studies *in vitro* demonstrated a critical role for SCF, with enhanced expansion of $CD133^+CD34^+$ cells using a minimal cocktail of SCF, TPO and Flt3L. Importantly, our *in silico* model allowed us to predict the influence of such cytokines on the survival, duplication and differentiation of the $CD133^+CD34^+$ HSC/HPCs.

Reaching these conclusions required laborious efforts to extract the main signaling pathways that are considered to play an important role in these processes. This extraction or, more appropriately,

the summation of these signaling pathways was required because an exhaustive model of a single biological pathway entails very complex models based on systems of tens to many thousands of equations; moreover in many cases, it includes unknowns that cannot be measured experimentally. We then proceeded to apply the old but effective approach sometimes referred to as the *lex parsimoniae ('the law of briefness')* or most commonly known as the *Ockam's Razor*, '*Pluralitas non est ponenda sine necessitate*'. In very simple words, in the description of a phenomenon, the most useful model is the one where more entities are not used than are necessary. In this regard, following up the above example for a minimal cytokine cocktail, we used the most important elements gathered both from the literature and from experimental evidence to develop an ODE model. The final model revealed that by adding IL-6 and FGF-1 to the minimal cytokine cocktail described above (i.e. SCF+IL-6+TPO+Flt3L+FGF-1; Fig. 3C), we could achieve the main two targets for our model, i.e. preserving or enhancing $CD133^+CD34^+$ cell numbers while using the minimum number of cytokines to generate the highest $CD133^+CD34^+$ cell expansion based on the cytokines selected for study. The prediction was confirmed *in vitro*, ratifying the ability of the model to be used as an *in silico* lab to study the effects of cytokine cocktails on $CD133^+CD34^+$ cells. One advantage of the *in silico* generated protocols compared with more traditional *in vitro* derived 'trial and error' protocols relates to the reduction in the cost of wet lab experiments even though initially there has been a significant investment in time in collecting and integrating specialized information into a set of differential equations.

On the other hand, the model has limitations. One of these is that not all the effects of combined cytokines can be reproduced by the *in silico* model as some of them are not known or disputed or not clear. Second, we restricted the first iteration of our model to $CD133^+CD34^+$ HSC/HPC and further iterations will need to analyze subsets of these cells for specific effects of cytokines and small molecules on the expansion of long term durable repopulating HSCs and their committed multipotent progenitor cells. Indeed, the model allows us to concentrate our attention on those biological events that are useful to investigate, for example new interactive or epigenetic mechanisms that also influence stem cells dynamics. An additional limit of the study is that it is entirely based on *in vitro* data. Thus, combining our approach with reliable preclinical *in vivo* models will confirm and predict optimal expansion protocols for both enhancing the short and longer term repopulating cells that are needed for reducing the morbidity and mortality associated with HSC transplantation.

Funding

This work was supported by NHS Blood and Transplant, the NHSBT Trust Fund and the National Institute for Health Research. This article summarizes independent research supported by the National Institute for Health Research (NIHR) to S.M.W. under its Programme Grants for Applied Research Programme (Grant Reference Number RP-PG-0310-1003).

Conflict of Interest: none declared.

References

Avery,S. *et al.* (2011) Influence of infused cell dose and HLA match on engraftment after double-unit cord blood allografts. *Blood*, **117**, 3277–3285.

Ballen,K.K. *et al.* (2013) Umbilical cord blood transplantation: the first 25 years and beyond. *Blood*, **122**, 491–498.

Benveniste,P. *et al.* (2014) Notch signals are required for *in vitro* but not *in vivo* maintenance of human hematopoietic stem cells and delay the appearance of multipotent progenitors. *Blood*, **123**, 1167–1177.

Boitano,A.E. *et al.* (2010) Aryl hydrocarbon receptor antagonists promote the expansion of human hematopoietic stem cells. *Science*, **329**, 1345–1348.

Camporeale,A. *et al.* (2003) Critical impact of the kinetics of dendritic cells activation on the *in vivo* induction of tumor-specific T lymphocytes. *Cancer Res.*, **63**, 3688–3694.

Castiglione,F. *et al.* (2012) A modeling framework for immune-related diseases. *Math. Model. Nat. Phenom.*, **7**, 40–48.

Chaurasia,P. *et al.* (2014) Epigenetic reprogramming induces the expansion of cord blood stem cells. *J. Clin. Invest.*, **124**, 2378–2395.

Cheung,A.M. *et al.* (2012) Distinct but phenotypically heterogeneous human cell populations produce rapid recovery of platelets and neutrophils after transplantation. *Blood*, **119**, 3431–3439.

Cheung,A.M. *et al.* (2013) Analysis of the clonal growth and differentiation dynamics of primitive barcoded human cord blood cells in NSG mice. *Blood*, **122**, 3129–3137.

Chiacchio,F. *et al.* (2014) Agent-based modeling of the immune system: NetLogo, a promising framework. *Biomed. Res. Int.*, **2014**, article id 907171.

Csaszar,E. *et al.* (2012) Rapid expansion of human hematopoietic stem cells by automated control of inhibitory feedback signaling. *Cell Stem Cell*, **10**, 218–229.

Csaszar,E. *et al.* (2014) Real-time monitoring and control of soluble signaling factors enables enhanced progenitor cell outputs from human cord blood stem cell cultures. *Biotechnol. Bioeng.*, **111**, 1258–1264.

Dahlberg,A. *et al.* (2014) Enhanced generation of cord blood hematopoietic stem and progenitor cells by culture with StemRegenin1 and Delta1 (Ext-IgG.). *Leukemia*, **28**, 2097–2101.

Danby,R. and Rocha,V. (2014) Improving engraftment and immune reconstitution in umbilical cord blood transplantation. *Front. Immunol.,* **5**, 1–19.

De Bruyn,C. *et al.* (2005*) Ex vivo* expansion of megakaryocyte progenitor cells: cord blood versus mobilized peripheral blood. *Stem Cells Dev.,* **14**, 415–424.

De Haan,G. (2003) *In vitro* generation of long-term repopulating hematopoietic stem cells by fibroblast growth factor-1. *Development*, **4**, 241–251.

Delaney,C. *et al.* (2013) Cord blood graft engineering. *Biol. Blood Marrow Transplant.*, **19** (1 Suppl.), S74–S78.

Drake,A.C. *et al.* (2011) Human CD34+ CD133+ hematopoietic stem cells cultured with growth factors including Angptl5 efficiently engraft adult NOD-SCID Il2rγ-/- (NSG) mice. *PLoS One*, **6**, e18382.

Faloon,P. *et al.* (2000) Basic fibroblast growth factor positively regulates hematopoietic development. *Development,* **127**, 1931–1941.

Fares,I. *et al.* (2014) Cord blood expansion. Pyrimidoindole derivatives are agonists of human hematopoietic stem cell self-renewal. *Science*, **345**, 1509–1512.

Fonseca-Pereira,D. *et al.* (2014) The neurotrophic factor receptor RET drives haematopoietic stem cell survival and function. *Nature*, **514**, 98–101.

Fuchs,E. *et al.* (2013) Alternative transplant donor sources: is there any consensus? *Curr. Opin. Oncol.*, **25**, 173–179.

Germain,R.N. *et al.* (2011) Systems biology in immunology: a computational modeling perspective. *Annu. Rev. Immunol.*, **29**, 527–585.

Goergens,A. *et al.* (2013) Revision of the human hematopoietic tree: granulocyte subtypes derive from distinct hematopoietic lineages. *Cell Rep.*, **3**, 1539–1552.

Gu,A. *et al.* (2014) Engraftment and lineage potential of adult hematopoietic stem and progenitor cells is compromised following short-term culture in the presence of an aryl hydrocarbon receptor antagonist. *Hum. Gene Ther. Methods*, **25**, 221–231.

Hagedorn,E.J. *et al.* (2014) Getting more for your marrow: boosting hematopoietic stem cell numbers with PGE2. *Exp. Cell Res.*, **4827**, 321–328.

Haylock,D.N. *et al.* (1997) Increased recruitment of hematopoietic progenitor cells underlies the *ex vivo* expansion potential of FLT3 ligand. *Blood*, **90**, 2260–2272.

Horwitz,M.E. *et al.* (2014) Umbilical cord blood expansion with nicotinamide provides long-term multilineage engraftment. *J. Clin. Invest.,* **124**, 3121–3128.

Kim,S. *et al.* (2014) Dynamics of HSPC repopulation in nonhuman primates revealed by a decade-long clonal-tracking study. *Cell Stem Cell*, **14**, 473–485.

Koller,M.R. *et al.* (1996) Flt-3 ligand is more potent than c-kit ligand for the synergistic stimulation of *ex vivo* hematopoietic cell expansion. *J. Hematother.*, **5**, 449–459.

Lee,J.A. *et al.* (2008) MIFlowCyt: the minimum information about a flow cytometry experiment. *Cytometry A,* **73,** 926–930.

Lemarie,C. *et al.* (2007) CD34 + progenitors are reproducibly recovered in thawed umbilical grafts, and positively influence haematopoietic reconstitution after transplantation. *Bone Marrow Transplant.*, **39**, 453–460.

Mendelson,A. and Frenette,P.S. (2014) Hematopoietic stem cell niche maintenance during homeostasis and regeneration. *Nat. Med.,* **20**, 833–846.

Migliaccio,A.R. *et al.* (2000) Cell dose and speed of engraftment in placental/umbilical cord blood transplantation: graft progenitor cell content is a better predictor than nucleated cell quantity. *Blood,* **96,** 2717–2722.

Morrison,S.J. and Scadden,D.T. (2014) The bone marrow niche for haematopoietic stem cells. *Nature*, **505**, 27–334.

Ohmizono,Y. *et al.* (1997) Thrombopoietin augments *ex vivo* expansion of human cord blood-derived hematopoietic progenitors in combination with stem cell factor and flt3 ligand. *Leukemia,* **11**, 524–530.

Oostendorp,R.A. *et al.* (2008) Oncostatin M-mediated regulation of KIT-ligand-induced extracellular signal-regulated kinase signaling maintains hematopoietic repopulating activity of Lin-CD34+CD133+ cord blood cells. *Stem Cells,* **26**, 2164–2172.

Notta,F. *et al.* (2011) Isolation of single human hematopoietic stem cells capable of long-term multilineage engraftment. *Science* **333**, 218–221.

Page,K.M. *et al.* (2011) Total colony forming units are a strong, independent predictor of neutrophil and platelet engraftment after unrelated umbilical cord blood transplantation: a single-center analysis of 435 cord blood transplants. *Biol. Blood Marrow Transplant.*, **17**, 1362–1374.

Pappalardo,F. *et al.* (2014b) Induction of T-cell memory by a dendritic cell vaccine: a computational model. *Bioinformatics*, **30**, 1884–1891.

Pappalardo,F. *et al.* (2015) Computational modelling approaches to vaccinology. *Pharmacol. Res.*, **92**, 40–45.

Pepperell,E.E. and Watt,S.M. (2013) A novel application for a 3D timelapse assay that distinguishes chemotactic from chemokinetic responses of hematopoietic CD133(+) stem/progenitor cells. *Stem Cell Res.,* **11**, 707–720.

Piacibello,W. *et al.* (1997) Extensive amplification and self-renewal of human primitive hematopoietic stem cells from cord blood. *Blood,* **89**, 2644–2653.

Rappold,I. *et al.* (1999) Gp130-signaling synergizes with FL and TPO for the long-term expansion of cord blood progenitors. *Leukemia*, **13**, 2036–2048.

Scaradavou,A. *et al.* (2010) Cord blood units with low CD34 + cell viability have a low probability of engraftment after double unit transplantation. *Biol. Blood Marrow Transplant.*, **16**, 500–508.

Scaradavou,A. *et al.* (2013) Double unit grafts successfully extend the application of umbilical cord blood transplantation in adults with acute leukemia. *Blood*, **121**, 752–758.

Shurin,M.R. *et al.* (1998) FLT3: receptor and ligand. Biology and potential clinical application. *Cytokine Growth Factor Rev.,* **9**, 37–48.

Takahashi,M. *et al.* (2014) CD133 is a positive marker for a distinct class of primitive human cord blood-derived CD34-negative hematopoietic stem cells. *Leukemia,* **28**, 1308–1315.

Tarasova,A. *et al.* (2011) Principal signalling complexes in haematopoiesis: structural aspects and mimetic discovery. *Cytokine Growth Factor Rev.*, **22**, 231–253.

van der Garde,M. *et al.* (2014) Thrombopoietin treatment of one graft in a double cord blood transplant provides early platelet recovery while contributing to long-term engraftment in NSG mice. *Stem Cells Dev.,* in press, doi:10.1089/scd.2014.0294.

Wagner,J.E. *et al.* (2002) Transplantation of unrelated donor umbilical cord blood in 102 patients with malignant and nonmalignant diseases: influence of CD34 cell dose and HLA disparity on treatment-related mortality and survival. *Blood*, **100**, 1611–1618.

Watt,S.M. (2014) Umbilical cord blood banking. In: Caplan,M.J. (ed.) *Reference Module in Biomedical Sciences*. Elsevier Press, Kidlington, UK, article 04238.

Watts,K.L. *et al.* (2013) CD34(+) expansion with Delta-1 and HOXB4 promotes rapid engraftment and transfusion independence in a *Macaca nemestrina* cord blood transplant model. *Mol. Ther.*, **21**, 1270–1278.

Wu,C. *et al.* (2014) Clonal tracking of Rhesus Macaque hematopoiesis highlights a distinct lineage origin for natural killer cells. *Cell Stem Cell*, **14**, 486–499.

Zhang,C.C. *et al.* (2008) Angiopoietin-like 5 and IGFBP2 stimulate *ex vivo* expansion of human cord blood hematopoietic stem cells as assayed by NOD/SCID transplantation. *Blood*, **111**, 3415–3423.